


Cite this: *RSC Adv.*, 2017, 7, 30979

# Ammonia-modulated reversible gel–solution phase transition and fluorescence switch for a salicylhydrazide-based metal–organic gel†

Shu-Mei Lu,<sup>‡a</sup> Jian-Cai Huang,<sup>‡a</sup> Guo-Ting Liu,<sup>a</sup> Zhi-Wei Lin,<sup>b</sup> Yan-Tong Li,<sup>a</sup> Xi-He Huang,<sup>id</sup><sup>a</sup> Chang-Cang Huang<sup>a</sup> and Shu-Ting Wu<sup>id</sup><sup>\*ac</sup>

Based on a multi-dentate salicylhydrazide-derived ligand, a Zn-contained metal–organic gel that could stand for months has been prepared. The driving force within the supramolecular assembly was discussed by studying the gelation conditions, optical spectra, dynamic rheology and mass spectra. These studies revealed that both the coordination bonds and hydrogen bonds participate in the supramolecular assembly. In addition, electrostatic force also played as a key role in stabilizing the gel phase. The charge nature of the colloidal particle is negative charged. Consequently, the xerogel shows significant adsorption behavior that favors positively charged dye molecules, such as methyl violet and methylene blue. The title gel exhibits gelation-induced fluorescence enhancement property. When the gel was exposed to ammonia vapor, a gel–solution transition occurred, accompanied by a great weakening of fluorescence. The phase transition and fluorescence switching were found to be reversible for at least seven cycles. The mechanism involved was studied and discussed.

Received 1st March 2017

Accepted 6th June 2017

DOI: 10.1039/c7ra02551c

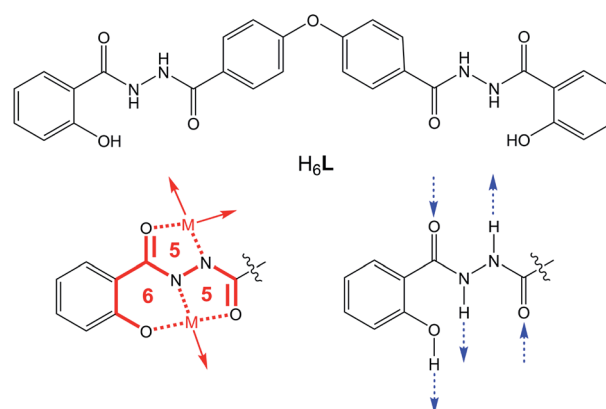
rsc.li/rsc-advances

## Introduction

In the last few decades, metal–organic gels (MOGs) have attracted much attention in the applications of optical materials,<sup>1</sup> sensing,<sup>1,2</sup> stimulate responsiveness,<sup>3</sup> self-healing,<sup>4</sup> redox,<sup>5</sup> chiral materials,<sup>6</sup> drug delivery,<sup>7</sup> catalysis,<sup>8</sup> adsorption and separation<sup>9</sup> *etc.* The advantages of MOGs include the rational design of the organic ligand, the properties of metal ions, and the processability of soft materials. By adopting the concept of supramolecular self-assembly to fabricate a MOG, coordination bonding is of key importance. The organic ligand always plays the role of a low molecular weight gelator (LMWG).<sup>10</sup> By exploring the reported functional MOGs, the structures of LMWGs share common characteristics as follows: (i) multiple coordination sites for multiple metal bindings, sometimes chelated;<sup>11</sup> (ii) certain function groups for molecular

interaction, such as amides for hydrogen bonding,<sup>12</sup> aromatic groups for  $\pi\cdots\pi$  stacking,<sup>13</sup> aliphatic groups for hydrophobic–hydrophilic interaction;<sup>14</sup> (iii) precise balance between the structural rigidity and flexibility to benefit both the minimum gelation concentration (MGC) and tunable properties.<sup>10,15</sup>

Herein, a multidentate salicylhydrazide derivative  $H_6L$  (Scheme 1) was synthesized and studied as a LMWG to form a Zn-contained MOG. The protons of the hydrazine and phenolic hydroxyl groups in salicylhydrazide ligand are apt to be released when  $H_6L$  reacts with transition metal ions in the DMF solution. The typical coordination mode reported is edge sharing 5-5-6 chelated rings (Scheme 1).<sup>16</sup> This chelated



**Scheme 1** The structure of  $H_6L$  (up) and the popular coordination mode and hydrogen bonding mode (down).

<sup>a</sup>Institute of Optical Crystalline Materials, College of Chemistry, Fuzhou University, Fuzhou, 350116, PR China. E-mail: shutingwu@fzu.edu.cn

<sup>b</sup>College of Chemistry and Chemical Engineering, Xiamen University, Xiamen 361005, PR China

<sup>c</sup>State Key Laboratory of Structural Chemistry, Fujian Institute of Research on the Structure of Matter, Chinese Academy of Sciences, Fuzhou, Fujian 350002, PR China

† Electronic supplementary information (ESI) available: Part I: experimental details including synthesis of the ligand  $H_6L$ , preparation of Gel2/1, dye adsorption tests, cycling experiments of the fluorescence sensing for  $NH_3$  and measurement details. Part II: synthesis and characterization of  $H_6L$  and Gel2/1 including the  $^1H$  NMR and mass spectra, IR spectra, dynamic rheology and high resolution mass spectrum. See DOI: 10.1039/c7ra02551c

‡ Shu-Mei Lu and Jian-Cai Huang are co-first authors.



coordination geometry is fairly stable in either solution or crystalline phase.<sup>17</sup> Secondly, as shown in Scheme 1, the salicylhydrazide group is a good candidate for hydrogen bonding in the supramolecular self-assembly. Thirdly, the two salicylhydrazides groups are spaced by a 4,4'-biphenyl oxide group. Thus the ligand might exhibit certain flexibility. In our previous study,<sup>18</sup> when the two salicylhydrazide groups are spaced by a 2,2'-biphenyl group, the ligand adopts typical 5-5-6 chelated coordination geometries with cupric ion. By the linkage of 2,2'-biphenyl group, there exists a common trinuclear coordination unit in several crystal structures.

In this paper, the gelation of the ligand  $H_6L$  was observed by the involvement of  $Zn^{2+}$  ion in DMF solution, showing interesting properties, such as gelation-induced fluorescence enhancement, reversible gel-solution transition, fluorescence switch, and selective dye adsorption. The characterization of the gel, as well as the intrinsic mechanism of properties were studied and discussed.

## Results and discussion

The synthesis and characterization of  $H_6L$  were described in the ESI† Typical gelation could be observed in 1 mL DMF solution that contains  $H_6L$  (0.0125 mmol) and  $Zn(OAc)_2$  (0.0250 mmol). When the concentration is higher, gelation occurs but serving mash-like gel; when the concentration is lower, the resultant looks like viscous fluid. Consequently, the MGC of the gel is *ca.* 1.2 wt%. In this concentration, transparent gel phase could be observed when the Zn/L molar ratio equal to 0.5/1, 1/1, 2/1 and 3/1 respectively (labelled as Gelx/1 respectively,  $x = 0.5, 1, 2, 3$ ) as shown in Fig. 1a. When the ratio is 4/1, no gelation occurs. In the Gelx/1 series, Gel2/1 shows the most stable gel phase that could maintain uniform gel phase for months, while Gel3/1 shows liquid extrusion after standing for several days, Gel0.5/1 and Gel1/1 exhibit too soft phase that easily deformed upon staying overnight.

As discussed above, the salicylhydrazide group tends to fully deprotonated to adopt the thermodynamic stable 5-5-6 chelated rings when it coordinates with transition metal ion.<sup>16</sup> For Gel3/1, the Zn/L ratio is equal to the charge ratio of  $L^{6-}$  and  $Zn^{2+}$  ion, so there is good chance for the coordination assembly to occur

in the system. The liquid extrusion effect of Gel3/1 suggests the coordination bonding is too strong to maintain an open network for trapping solvent molecules. When Zn/L ratio is lower, such as 2/1, the amount of metal ion is not enough for the coordination with  $L^{6-}$ . Excess  $H_6L$  may form hydrogen bonding to participate the supramolecular assembly. Considering the Gel2/1 is stable for months, the synergistic effect of coordination bonding and hydrogen bonding in Gel2/1 benefits the gel phase stabilization. When the Zn/L ratio is lower than 2/1, such as 0.5/1 and 1/1, the resulting gels become too soft to trap the solvent molecules, which suggests the hydrogen bonding assembly is not strong enough for obtaining the supramolecular network. On the other hand, when Zn/L ratio is 4/1, the remnant zinc ion might exist as solvated ion that brings in excess free positive charged particles, which make the system become solution. Thus the colloid particles in the gel may be negative charged.

To characterize the gel system, UV-Vis absorption spectra were taken. The spectrum of  $H_6L$  (red curve in Fig. 1b) shows typical absorption bands for  $\pi \rightarrow \pi^*$  and  $n \rightarrow \pi^*$ . Upon the addition of  $Zn^{2+}$  ion (Zn/L: 0.5/1–3/1), the charge transfer band (280–400 nm) greatly strengthen, which suggests the coordination assembly occurs for Gelx/1 ( $x = 0.5, 1, 2, 3$ ). When the equivalent of zinc ion increases from 0.5 to 3 eq., the absorbance at 339 nm increases. When the zinc ion' equivalent increases to 4 eq. or 6 eq., the absorbance at 339 nm doesn't change. These studies indicate the absorption band at 339 nm should be attributed to coordination bonding. IR spectra for zinc acetate,  $H_6L$  and Gel2/1 (Fig. S4 in ESI†) were recorded to study the coordination between  $H_6L$  and zinc ion. The 3309 ( $\nu_{OH}$ ) and 3046 ( $\nu_{NH}$ )  $cm^{-1}$  peaks of  $H_6L$  greatly weaken in the curve of Gel2/1, which indicates the proton loss of the  $H_6L$  in Gel2/1. By comparing with the spectra of zinc acetate,  $H_6L$  and Gel2/1 in the range of 1800–1200  $cm^{-1}$ , the red shift of  $\nu_{C=O}$  (from 1666  $cm^{-1}$  in  $H_6L$  curve to 1650  $cm^{-1}$  in Gel2/1 curve, the  $\nu_{C=O}$  in zinc acetate curve is at 1536  $cm^{-1}$ ) suggests the coordination between  $H_6L$  and zinc ion may occur. MALDI-MS (Matrix Assisted Laser Desorption Ionization Mass) spectrum for Gel2/1 reveals the possible self-assembly fashion. As shown in Fig. 2a, there exists wave-like spectrum line in the range of  $m/z$

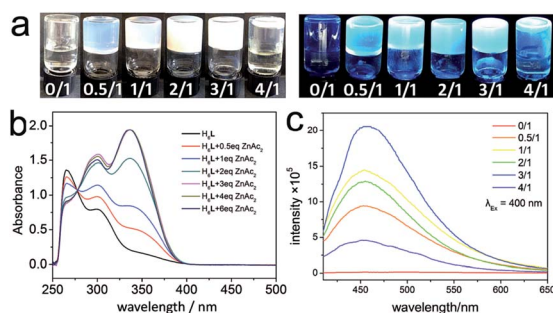


Fig. 1 (a) Photos of gelation test in different Zn/L molar ratios under daylight (left) and UV-lights (right). The UV-Vis absorption spectra (b) and fluorescence spectra (c) of the samples with diverse Zn/L molar ratio.

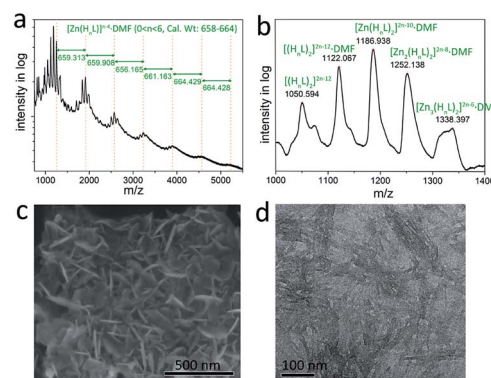


Fig. 2 (a and b) MALDI-MS spectra in the range of  $m/z$  750–5500 (a) and 1000–1400 (b) for Gel2/1. (c and d) FESEM (c) and TEM (d) micrograph of Gel2/1.



$z$  1000–5000 with regular intervals that closed to the molecular weight of  $[\text{Zn}(\text{H}_n\text{L})]^{n-4} \cdot \text{DMF}$  ( $0 < n < 6$ , calc. wt: 658–664). The strongest peaks in the range of  $m/z$  1000–1400 could be attributed to the assembly of two  $\text{H}_n\text{L}$  ( $0 < n < 6$ ) molecules with certain equivalents of  $\text{Zn}^{2+}$  ion and DMF molecule (Fig. 2b). Consequently, the self-assembly between  $\text{H}_6\text{L}$  and  $\text{Zn}^{2+}$  ion involved in Gel2/1 is assumed to follow a step-by-step style driven by the synergistic effect of coordination assembly and hydrogen bonding. The microscopic morphology of Gel2/1 is studied by FESEM and TEM, showing thin sheets in nanoscale (Fig. 2c and d).

As shown in Fig. 1a, blue light emission could be observed by keeping Gel $x$ /1 ( $x = 0.5, 1, 2, 3$ ) sample under UV light in the dark room. By using fluorescence spectrometer, the gel samples could emit fluorescence under the excitation of 400 nm (Fig. 1c). The emission intensity increases along with the Zn/L from 0.5/1 to 3/1. While for the Zn/L = 4/1 sample, the emission intensity greatly weakens along with the destruction of gel phase, which indicates gelation-induced fluorescence enhanced effect. Further dynamic rheology performed on Gel2/1 suggests the gel has a certain rigidity, with storage modulus  $G'$  about 10 times larger than the loss modulus  $G''$  within the frequency 0.01–10 Hz (Fig. S5 in ESI†). In this context, the gelation-induced fluorescence enhanced effect could be due to the rigidification upon gelation that slows down non-radiative decay processes.<sup>10a</sup> Besides that, rheological measurements also shows a small critical strain (0.1%), indicating Gel2/1 may be an electrostatically stabilized system. To study the charge property of Gel2/1, NaCl,  $\text{MgCl}_2$  and  $\text{AlCl}_3$  aqueous solution were layered onto the gel phase. After leaving the testing gel in room temperature for one hour, the gel which treated with  $\text{AlCl}_3$  aqueous solution completely dissolved into clear solution, the gel that treated with  $\text{MgCl}_2$  aqueous solution partly dissolved. While the NaCl solution seems to do not influence the gel status. In that case, the colloidal particle in Gel2/1 should be negative charged. The electrostatic force plays an important role to stabilize the gel system.

The relationship among the supramolecular structure, phase status and photoluminescence property were studied by introducing ammonia vapour. On one hand, ammonia vapour is a kind of basic gas that could influence the coordination bonding in some extent, and be easy to evaporate to allow a promising reversible modulation. On the other hand,  $\text{NH}_3$  molecule is a good candidate for hydrogen bonding. As shown in Fig. 3a, upon exposing in the ammonia vapour, the gel (labelled as Gel<sup>O</sup>, where subscribe “O” means original) becomes transparent light yellow solution (labelled as Solution<sup>C1</sup>, where subscribe “C1” means the first cycle), and the fluorescence greatly weakens. After the  $\text{NH}_3$  evaporates naturally, transparent gel phase reforms in two days, and the photoluminescence enhances again (labelled as Gel<sup>C1</sup>). Emission spectra for Gel2/1 sample were recorded to study this phenomenon. As shown in Fig. 3b, the initial emission spectrum for original Gel2/1 (Gel<sup>O</sup>) exhibits strong peak at 447 nm. After the phase transition completes, the emission intensity of the solution with the involvement of  $\text{NH}_3$  (Solution<sup>C1</sup>) is closed to zero (grey curve in Fig. 3b). Repeated tests for 7 cycles of Gel2/1 sample suggest that the fluorescence on and off effect is reversible along with

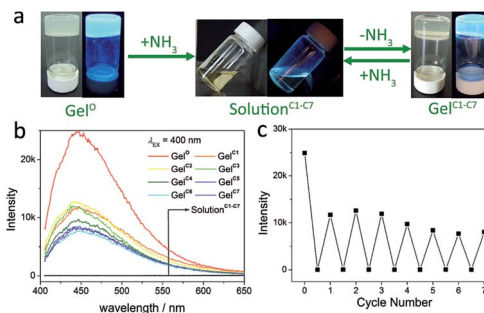


Fig. 3 (a) Scheme of the reversible gel-solution phase transition. (b) The emission spectra of Gel2/1 sample in gel-solution phase transition that induced by  $\text{NH}_3$  gas. The colourful curves represent samples of Gel<sup>O</sup> and Gel<sup>C1-C7</sup>, the grey curves represent samples of Solution<sup>C1-C7</sup>. (c) The relationship between fluorescence intensity at 447 nm and the cycle number of phase transition of Gel2/1 sample.

the phase transformation. However, it should be pointed out that the fluorescence intensity of the gel in cycle 1–7 (Gel<sup>C1-C7</sup>) was lower than the original gel sample (Gel<sup>O</sup>), ca. 51–31%, which might be due to the residue  $\text{NH}_3$  in the gel sample.

To discuss the possible mechanism of the phase transition, the role of ammonia becomes important. It was found that the complete phase transition from gel to solution required only 5 minutes. When the Gel2/1 has been in the ammonia vapour for just 1 minute, the gel phase becomes so soft that closed to the colloidal sol phase. The UV-Vis absorption spectrum for three states, (1) the gel, (2) solution and (3) the intermediate soft colloidal sol, were recorded. As shown in Fig. S6,† the absorption spectra for state 1–3 are similar, which indicate ammonia vapour may not disrupt the coordination of  $\text{H}_6\text{L}$  to zinc ion significantly.

Furthermore, HRMS-ESI spectra for state 3 and state 4 (in this case, the initial gel solution was allowed to stay for 5 min after mixing reactants, then diluted in acetonitrile for mass study) were tested. As shown in Fig. S7† (state 3), there are anion  $m/z = 1051.2930$  ( $[\text{H}_6\text{L} \cdot \text{H}_5\text{L}]^-$  calc. 1051.2904), anion  $m/z = 1113.2063$  ( $[\text{Zn} \cdot \text{H}_5\text{L} \cdot \text{H}_4\text{L}]^-$  calc. 1113.2039), indicating the ligands can aggregate with each other or aggregate with  $\text{Zn}^{2+}$  in the presence of ammonia. Fig. S8 and S9† for state 4 suggest that small aggregates already exist in the first 5 min of gelation. There are cation  $m/z = 1115.2157$  ( $[\text{Zn} \cdot \text{H}_6\text{L} \cdot \text{H}_5\text{L}]^+$  calc. 1115.2190), cation  $m/z = 1579.4511$  ( $[\text{H}_6\text{L} \cdot \text{H}_5\text{L}]^+$  calc. 1579.4544), anion  $m/z = 1014.2029$  ( $z = 3$ ) ( $[\text{H}_6\text{L} \cdot \text{H}_5\text{L} \cdot \text{H}_4\text{L}]^3-$  calc. 1014.7386). By comparing the HRMS-ESI spectra of state 3 and 4, it is speculated that the introduction of ammonia may hinder the assembly of small aggregates into larger one. In other words, the supramolecular network in Gel2/1 that dealt with ammonia would be cut into pieces that no longer hold the solvent molecules. In that case, the gel-solution phase transition was observed.

To explore the application of Gel2/1, four charged dye molecules were tested by the adsorption of the xerogel sample for Gel2/1. The experimental details were described in ESI-1.3.† As shown in Fig. 4, the solution of positively charged methyl violet and methylene blue exhibit significant adsorption behavior upon the xerogel of Gel2/1, while, there is no evidence





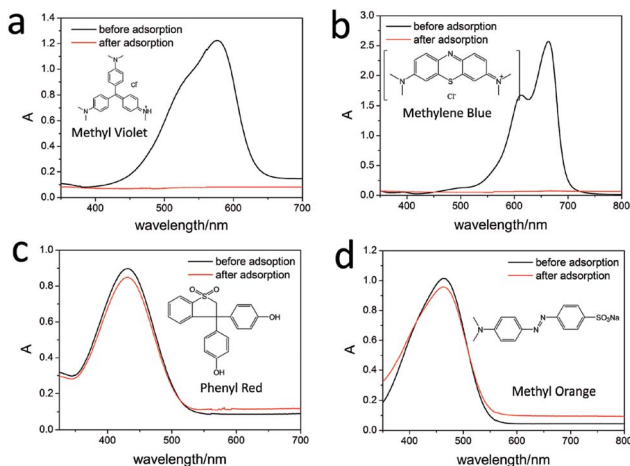


Fig. 4 The selective adsorption behavior for Gel2/1 in the presence of methyl violet (a), methylene blue (b), phenyl red (c) and methyl orange (d), respectively.

for the negatively charged phenyl red and methylene orange solution be absorbed by the xerogel. The results shown that the xerogel could significant absorb positive charged dye molecules, which is consistent with the electrolyte experiments that discussed above.

## Conclusions

In summary, a metal–organic gel based on  $\text{Zn}^{2+}$  and salicylhydrazide-derived ligand  $\text{H}_6\text{L}$  has been developed, showing significant gelation-induced fluorescence enhancement. Discussion around the driving force of supramolecular assembly inspires the study of modulation over material phase and photoluminescence. Ammonia vapour is found to successfully change the material phase from gel to solution. Reversible phase transition and fluorescence on–off switch were observed by the introduction and evaporation of  $\text{NH}_3$ . The mechanism of the phase transition is discussed.

## Acknowledgements

We thank the financial support from the National Natural Science Foundation of China (21671041), the Foundation of Educational Commission of Fujian Province (JA14056), the Natural Science Foundation of Fujian Province (2016J01688), the State Key Laboratory of Structural Chemistry, Fujian Institute of Research on the Structure of Matter, CAS (20160010), the Science and Technology Development Funding of Fuzhou University (2014-XQ-10). We thank Prof. Zhao's lab in Fuzhou University for technical support.

## Notes and references

- 1 P. Chen, Q. Li, S. Grindy and N. Holten-Andersen, *J. Am. Chem. Soc.*, 2015, **137**, 11590–11593.
- 2 (a) C. D. Jones and J. W. Steed, *Chem. Soc. Rev.*, 2016, **45**, 6546–6596; (b) Q. Li, T.-T. Lu, X. Zhu, T.-B. Wei, H. Li and

- Y.-M. Zhang, *Chem. Sci.*, 2016, **7**, 5341–5346; (c) Q. Lin, T.-T. Lu, X. Zhu, B. Sun, Q.-P. Yang, T.-B. Wei and Y.-M. Zhang, *Chem. Commun.*, 2015, **51**, 1635–1638.
- 3 (a) T.-T. Lu, J. Liu, H. Li, T.-B. Wei, Y.-M. Zhang and Q. Lin, *Progr. Chem.*, 2016, **28**, 1541–1549; (b) Y. Liu, Y. Wang, L. Jin, T. Chen and B. Yin, *Soft Matter*, 2016, 934–945; (c) A. J. McConnell, C. S. Wood, P. P. Neelakandan and J. R. Nitschke, *Chem. Rev.*, 2015, **115**, 7729–7793; (d) M. Martínez-Calvo, O. Kotova, M. E. Möbius, A. P. Bell, T. McCabe, J. J. Boland and T. Gunnlaugsson, *J. Am. Chem. Soc.*, 2015, **137**, 1983–1993.
- 4 (a) T. Feldner, M. Häring, S. Saha, J. Esquena, R. Banerjee and D. D. Díaz, *Chem. Mater.*, 2016, **28**, 3210–3217; (b) M. Martínez-Calvo, O. Kotova, M. E. Möbius, A. P. Bell, T. McCabe, J. J. Boland and T. Gunnlaugsson, *J. Am. Chem. Soc.*, 2015, **137**, 1983–1993; (c) L. Yan, S. Gou, Z. Ye, S. Zhang and L. Ma, *Chem. Commun.*, 2014, **50**, 12847–12850.
- 5 (a) S. Bhattacharya and S. K. Samanta, *Chem. Rev.*, 2016, **116**, 11967–12028; (b) B. Sharma, A. Mahata, S. Mandani, T. K. Sarma and B. Pathak, *RSC Adv.*, 2016, **6**, 62968–62973; (c) M. Paul, K. Sarkar and P. Dastidar, *Chem.–Eur. J.*, 2015, **21**, 255–268; (d) S. Shi, Q. Wang, T. Wang, S. Ren, Y. Gao and N. Wang, *J. Phys. Chem. B*, 2014, **118**, 7177–7186.
- 6 (a) X. Zhou, Q. Jin and L. Zhang, *Small*, 2016, **12**, 4743–4752; (b) Z. Shen, T. Wang, L. Shi, Z. Tang and M. Liu, *Chem. Sci.*, 2015, **6**, 4267–4272; (c) Z. Shen, Y. Jiang, T. Wang and M. Liu, *J. Am. Chem. Soc.*, 2015, **137**, 16109–16115.
- 7 (a) R. Langasco, G. Spada and S. T. Tanriverdi, *J. Pharm. Pharmacol.*, 2016, **68**, 999–1009; (b) S. Y. Tan, C. Y. Ang, A. Mahmood, Q. Qu, P. Li, R. Zou and Y. Zhao, *ChemNanoMat*, 2016, **2**, 504–508.
- 8 (a) L. Zeng, P. Liao, H. Liu, L. Liu, Z. Liang, J. Zhang, L. Chen and C.-Y. Su, *J. Mater. Chem. A*, 2016, **4**, 8328–8336; (b) B. G. Xing, M. F. Choi and B. Xu, *Chem.–Eur. J.*, 2002, **8**, 5028–5032.
- 9 (a) B. O. Okesola and D. K. Smith, *Chem. Soc. Rev.*, 2016, **45**, 4226–4251; (b) J. Sui, L. Wang, W. Zhao and J. Hao, *Chem. Commun.*, 2016, **52**, 6993–6996.
- 10 (a) P. Sutar and T. K. Maji, *Chem. Commun.*, 2016, **52**, 8055–8074; (b) P. Dastidar, S. Ganguly and K. Sarkar, *Chem.–Asian J.*, 2016, **11**, 2484–2498.
- 11 For examples, see: (a) A. M. Amacher, J. Puigmarti-Luis, Y. Geng, V. Lebedev, V. Laukhin, K. Kramer, J. Hauser, D. B. Amabilino, S. Decurtins and S.-X. Liu, *Chem. Commun.*, 2015, **51**, 15063–15066; (b) V. M. Suresh, A. De and T. K. Maji, *Chem. Commun.*, 2015, **51**, 14678–14681; (c) Y. Li, C. Zhou, L. Xu, F. Yao, L. Cen and G. D. Fu, *RSC Adv.*, 2015, **5**, 18242–18251.
- 12 For examples, see: (a) J.-L. Zhong, X.-J. Jia, H.-J. Liu, X.-Z. Luo, S.-G. Hong, N. Zhang and J.-B. Huang, *Soft Matter*, 2016, **12**, 191–199; (b) K. Nath, A. Husain and P. Dastidar, *Cryst. Growth Des.*, 2015, **15**, 4635–4645.
- 13 For examples, see: (a) X. Zhao, L. Yuan, Z.-Q. Zhang, Y.-S. Wang, Q. Yu and J. Li, *Inorg. Chem.*, 2016, **55**, 5287–5296; (b) S. Roy, A. K. Katiyar, S. P. Mondal, S. K. Ray and K. Biradha, *ACS Appl. Mater. Interfaces*, 2014, **6**, 11493–11501.



- 14 For examples, see the references in X. Du, J. Zhou, J. Shi and B. Xu, *Chem. Rev.*, 2015, **115**, 13165–13307.
- 15 For examples, see: (a) N. Luisier, R. Scopelliti and K. Severin, *Soft Matter*, 2016, **12**, 588–593; (b) R. D. Mukhopadhyay, V. K. Praveen, A. Hazra, T. K. Maji and A. Ajayaghosh, *Chem. Sci.*, 2015, **6**, 6583–6591.
- 16 Search by the salicylhydrazide group as the key molecular structure in CCDC database (up to 2016), there are 159 hits, including 147 hits whose structures exhibit 5-5-6 coplanar coordination chelated rings.
- 17 (a) F. Hengesbach, X. Jin, A. Hepp, B. Wibbeling, E.-U. Wuerthwein and W. Uhl, *Chem.-Eur. J.*, 2013, **19**, 13901–13909; (b) A. Trzesowska-Kruszynska, *Cryst. Growth Des.*, 2013, **13**, 3892–3900; (c) Z.-Z. Wen, X.-L. Wen, S.-L. Cai, S.-R. Zheng, J. Fan and W.-G. Zhang, *CrystEngComm*, 2013, **15**, 5359–5367; (d) P. Krishnamoorthy, P. Sathyadevi, R. R. Butorac, A. H. Cowley, N. S. P. Bhuvanesh and N. Dharmaraj, *Dalton Trans.*, 2012, **41**, 6842–6854; (e) A. Jamadar, A. K. Duhme-Klair, K. Vemuri, M. Sritharan, P. Dandawatec and S. Padhye, *Dalton Trans.*, 2012, **41**, 9192–9201; (f) M. J. Prakash and M. S. Lah, *Chem. Commun.*, 2009, 3326–3341; (g) D. Moon, J. Song and M. S. Lah, *CrystEngComm*, 2009, **11**, 770–776; (h) X. F. Liu, W. L. Liu, K. Lee, M. Park, H. C. Ri, G. H. Kimd and M. S. Lah, *Dalton Trans.*, 2008, 6579–6583; (i) D. Moon, K. Lee, R. P. John, G. H. Kim, B. J. Suh and M. S. Lah, *Inorg. Chem.*, 2006, **45**, 7991–7993; (j) S.-X. Liu, S. Lin, B.-Z. Lin, C.-C. Lin and J.-Q. Huang, *Angew. Chem., Int. Ed.*, 2001, **40**, 1084–1087.
- 18 S.-T. Wu, H.-L. Tang, S.-M. Lu, Q.-Y. Ye, X.-H. Huang, C.-C. Huang, X.-L. Hu and S.-T. Zheng, *CrystEngComm*, 2014, **16**, 9792–9799.

